ORIGINAL RESEARCH

LncRNA RP11-422N16.3 Inhibits Cell Proliferation and EMT, and Induces Apoptosis in Hepatocellular Carcinoma Cells by Sponging miR-23b-3p

Yunpeng Sun[1]
Qingqing Zhou[2]
Junjian Li[1]
Chang Zhao[1]
Zhengping Yu[1]
Qiandong Zhu[1]

[1]Departments of Hepatobiliary Surgery, The First Affiliated Hospital of Wenzhou Medical University, Wenzhou, Zhejiang 325000, People's Republic of China; [2]Departments of Nursing, The First Affiliated Hospital of Wenzhou Medical University, Wenzhou, Zhejiang 325000, People's Republic of China

Objective: This study investigated the mechanism of RP11-422N16.3 sponging miR-23b-3p in cell proliferation, apoptosis and epithelial-mesenchymal transition (EMT) in liver cancer.

Methods: Expressions of RP11-422N16.3, miR-23b-3p and dimethylglycine dehydrogenase (DMGDH) were determined in liver cancer tissues, adjacent normal tissues, hepatocellular carcinoma cell lines and normal liver epithelial cell line. Up-regulation of RP11-422N16.3 and down-regulation of miR-23b-3p were conducted in hepatocellular carcinoma cells. Bioinformatics analysis, luciferase reporter assay and RNA-pull down assay were performed to verify the relationship among miR-23b-3p, DMGDH, as well as RP11-422N16.3. Cell proliferation and cell apoptosis were determined by CCK-8 and Flow Cytometry analysis, respectively.

Results: Expressions of RP11-422N16.3 and DMGDH were down-regulated while that of miR-23b-3p were up-regulated in hepatocellular carcinoma cancer tissues and cells. RP11-422N16.3 localized in cytoplasm and competitively bound to miR-23b-3p. Up-regulation of RP11-422N16.3 and down-regulation of miR-23b-3p contributed to increased expressions of DMGDH and E-cadherin, and decreased expressions of miR-23b-3p, ZEB1, Snail and Vimentin, resulting in inhibiting cell proliferation and promoting cell apoptosis. Inhibition of RP11-422N16.3 or overexpression of miR-23b-3p accelerated cell proliferation and slowed down cell apoptosis. miR-23b-3p inhibited the expression of DMGDH.

Conclusion: Our data suggested that LncRNA RP11-422N16.3, by competitively binding to miR-23b-3p, promoted DMGDH expression, contributing to inhibit cell proliferation and EMT, and induce cell apoptosis in hepatocellular carcinoma cells.

Keywords: LncRNA RP11-422N16.3, DMGDH, miR-23b-3p, liver cancer, hepatocellular carcinoma

Introduction

Hepatocellular carcinoma is a common malignant tumor, and its incidence rate ranks fifth among tumor-related diseases, while its mortality accounts for the second place.[1] Currently, liver cancer treatment methods are extremely limited and the effect is poor. To date, there are not many approved liver cancer-related molecules reported in different laboratories around the world.[2] Therefore, only by further researching the pathogenesis of liver cancer, exploring new intervention strategies, and finding new diagnostic and therapeutic targets can we further improve the therapeutic effect on liver cancer.

Long non-coding RNA (LncRNA) is a type of RNA that does not encode a protein with a transcript of more than 200 nt in length. This kind of RNA was originally thought

Correspondence: Qiandong Zhu
Departments of Hepatobiliary Surgery, The First Affiliated Hospital of Wenzhou Medical University, Wenzhou, Zhejiang 325000, People's Republic of China
Tel +86-577-55579453
Email wzqdzhu@163.com

to be the "noise" of genomic transcription.[3] With the discovery of HOTAIR function in 2007, the function of lncRNA gradually became clear.[4] Although only a small number of lncRNA functions have been reported, it is clear that lncRNA is involved in the regulation of development, differentiation, metabolism and tumorigenesis and progression.[5] The expression of lncRNA HULC is abnormally elevated in pancreatic cancer, and its abnormally high expression is significantly associated with tumor volume, high-grade lymph node metastasis and vascular invasion, and HULC level is associated with overall patient survival.[6,7] HOTAIR is elevated in various cancers such as breast cancer,[8] colorectal cancer[9] and cervical cancer;[10] in cervical cancer, high expression of HOTAIR is associated with lymph node metastasis and patient overall survival rate is low;[11] Cell biology experiments showed that knockdown of HOTAIR can significantly inhibit the proliferation, migration and invasion of cervical cancer cells, while overexpression of HOTAIR can cause EMT-related phenotypes.[12] In our previous study, we screened lncRNAs that were significantly differentially expressed in liver cancer and closely related to prognosis based on large sample RNAseq bioinformatics data from the TCGA database to provide possible targets for targeted therapy. RP11-422N16.3 was one of them (Supplementary Figure 1). In addition, lncRNAs can also participate in gene transcriptional processes mediated by DNA methylation, acetylation, etc. to regulate tumorigenesis.[13] Although we have a significant increase in the understanding of lncRNAs, this is only the tip of the iceberg, the complex biological functions of lncRNAs in cancer, and the detailed regulation mechanism remains to be further studied.

The miRNA can be complementary to the target RNA, resulting in the restriction of gene expression and protein synthesis; and lncRNAs can directly or indirectly interact with the microRNA, causing it to lose its regulatory function.[14–16] The miR-23b-3p belongs to the miR-23b/27b/24–1 cluster and has been reported to function as an onco-miR in different cancers including glioma, gastric cancer, and breast cancer.[17,18] However, the functions and mechanisms of miR-23b-3p in hepatocellular carcinoma have not been previously reported.

In a study on liver cancer, it was confirmed that dimethylglycine dehydrogenase (DMGDH) can inhibit tumor metastasis by inhibiting Akt activation, and can be used as a biomarker to distinguish between benign and malignant tumors.[19] In addition, recent epidemiological studies have revealed that DMGDH deficiency may be involved in the progression of diabetes, further emphasizing the importance

of the enzyme.[20] We further studied through the UCSC website that RP11-422N16.3 was mapped to Human (GRCh38.p10) chr8 (q23.2), strand= +, with two exons and a transcript length of 3075 bps (Supplementary Figure 2A and B). Furthermore, multiple algorithms in the online database LNCipedia predicted that RP11-422N16.3 did not have protein-coding capability (Supplementary Figure 3). The DMGDH gene is located in Human (GRCh38.p10) chr5 (q14.1), strand= -. We obtained a promoter sequence of 2000bps upstream of the DMGDH gene. The analysis found that: RP11-422N16.3 chr8: 109,646,792–109,646,804 is 5′-CTTTTTTCTCTCTCA-3′, DMGDH promoter chr5:79,071,006–79,071,018 is 5′-TGAGAGAAAAAAG-3′, they can be reverse-complementary paired binding, with the basis of targeted regulation (Supplementary Figure 2C). Based on the results of previous studies and data analysis, we hypothesized that RP11-422N16.3 can positively regulate the expression of DMGDH gene by competitively binding to miR-23b-3p, thereby affecting the biological behaviors such as proliferation and metabolism of liver cancer cells, thus playing an important role in the occurrence and development of liver cancer.

Materials and Methods
Ethical Statement
This study was approved by the Ethics committee of The First Affiliated Hospital of Wenzhou Medical University. All patients signed written informed consents and had the right to know the experiment prior to the study.

Study Subjects
A total of 55 patients with hepatocellular carcinoma diagnosed from April 2016 to April 2019 in our hospital were included in this study. The hepatocellular carcinoma tissues and adjacent normal tissues (5 cm away from the cancer tissues) were collected. The inclusion criteria were 1) patients were pathologically diagnosed with hepatocellular carcinoma; and 2) no history of radiotherapy, chemotherapy and other adjuvant therapy. Subjects were eliminated from inclusion if they 1) had distant metastasis; 2) had other malignant tumors; and 3) were pregnant or lactating.

Cell Cultures
Hepatocellular carcinoma cell lines (HepG2, SMMC-7721, MHCC97-H, and HCCLM3) and human normal liver cell line (L02) were purchased from Shanghai Institutes for Biological Sciences, CAS (Shanghai, China). All cells were incubated in DMEM culture medium (Gibco, Grand Island,

NY, USA) which contains 10% FBS (Gibco, Grand Island, NY, USA) in an incubator at 37°C with 5% CO_2. The culture medium was replaced every 2 to 3 days. Sub-culture was conducted when cell density reaches 80–90%. The expressions of RP11-422N16.3 and miR-23b-3p in each cell lines were determined using qRT-PCR. The HepG2 cells showed the biggest difference of expressions of both RP11-422N16.3 and miR-23b-3p compared with normal epithelial cells and was selected for further experiments.

Cell Grouping and Corresponding Treatment

HepG2 cells at their logarithmic growth phase was divided into the following seven groups: 1) Blank group (no treatment), 2) pcDNA3.1 group (transfected with pcDNA3.1), 3) pcDNA3.1-RP11-422N16.3 group (transfected with pcDNA3. 1-RP11-422N16.3); 4) inhibitors NC group (negative control, transfected with inhibitors NC); 5) miR-23b-3p inhibitors group (transfected with miR-23b-3p inhibitors); 6) pcDNA3. 1-RP11-422N16.3+mimics NC group (transfected with pcDNA3.1-RP11-422N16.3 and mimics NC); and 7) pcDN A3.1-RP11-422N16.3+miR-23b-3p mimics group (transfected with pcDNA3.1-RP11-422N16.3 and miR-23b-3p mimics). pcDNA3.1, pcDNA3.1-RP11-422N16.3, inhibitors NC, miR-23b-3p inhibitors, mimics NC and miR-23b-3p mimics were purchased from Sangon Biotech (Shanghai, China). Cell transfection was conducted according to the instruction of Lipofectamine 2000 (Invitrogen, Carlsbad, CA, USA). Transfected cells were incubated for 48 hrs and subjected to morphology evaluation with an inverted microscope.

Determining the Localization of RP11-422N16.3 in Cells

PARISTM Kit (Ambion, Austin, Texas, USA) was used for subcellular fractionation. HepG2 cells were harvested, washed with PBS and put on ice. Then, 500 μL of pre-cold cell fractionation buffer was used to resuspend cells, followed by dissolution on ice for 10 min. After cells were centrifuged for 5 mins, the supernatant (cytoplasm) was separated from sediment (cell nucleus). The separated supernatant was added with same volume of 2 × Lysis/Binding Solution for full mixture to prevent RNA from degradation. Anhydrous alcohol of the same volume of supernatant was then added before the mixture was added into the filter candle of the kit. The liquid was abandoned after the filter candle was washed for several times. The RNA on the filter was collected, which was the dissolved cytoplasm RNA, by

centrifugation for 30s. Cell nucleus sediment was harvested based on process above, which was the final nucleus RNA. Then, cytoplasm RNA and nucleus RNA were collected for reverse transcript using M-MLV kit (No. 28025013. ThermoFisher Scientific, USA). Expressions of RP11-422N16.3 in cytoplasm and nucleus were determined using qRT-PCR.

Dual-Luciferase Reporter Assay

Bioinformatics software (http://www.targetscan.org) was used to predict the relationship of lncRNA RP11-422N16.3 and miR-23b-3p. Luciferase reporter assay was used to verify the relationship between lncRNA RP11-422N16.3 and miR-23b-3p. The artificially synthesized RP11-422N16.3 3′UTR gene sequence was introduced to pMIR-reporter (Beijing Huayue Biotechnology Co., Ltd, Beijing, China) through restriction enzyme sites Bamh1 and Ecor1. A mutant site of the complementary sequence of RP11-422N16.3 wide target sequence was designed and the target segment was inserted into the pMIR-reporter plasma through restriction enzyme digested T4 DNA. The confirmed WT and MUT plasmids were separately transfected with mimics NC and miR-23b-3p mimics into 293T cells (Shanghai Beinuo Bio-Tech Co., Ltd, Shanghai, China). Cells were harvested after being transfected for 48 hrs and subjected to cell lysis. Glomax20/20 luminometer (Promega, Madison, Wisconsin, USA) and Luciferase kit (BioVision, San Francisco, CA, USA) were used to detect the activity of luciferase. Experiments in each group were repeated three times.

Bioinformatics software (http://www.targetscan.org) was used to predict the relationship of miR-23b-3p and DMGDH, as well as the binding site of miR-23b-3p and DMGDH 3′UTR. The DMGDH 3′UTR promoter sequence with binding site of miR-23b-3p was synthesized to construct DMGDH 3′UTR wild type plasmid (DMGDH 3′UTR-WT). DMGDH 3′UTR mutant plasmid (DMGDH 3′UTR -MUT) was also constructed. The plasmid was established according to the procedure instructed on the plasmid extraction kit (Promega, Madison, Wisconsin, USA). Then, cells in the logarithmic phase were seeded into a 96-well plate and when cell density reached 70%, DMGDH 3′UTR-WT and DMGDH-3′UTR-MUT plasmids were respectively transfected with mimics NC and miR-23b-3p mimics into 223b-3pT cells using Lipofectamine 2000 regent. Cells were harvested after being transfected for 48 hrs and subjected to cell lysis.

Verifying the Relationship of RP11-422N16.3 and miR-23b-3p by RNA-Pull Down

A total volume of 50 nM miR-23b-3p transfected with biotin labeled WT and 50 nM of miR-23b-3p transfected with biotin labeled MUT were separately transfected into cells. After being transfected for 48 hrs, cells were harvested and washed with PBS before being incubated with special cell lysis buffer (Ambion, Austin, Texas, USA) for 10 mins. Then, 50 mL of cell lysates were prepared and incubated with M-280 strep-tavidin MagneSphere (Sigma, St. Louis, MO, USA) pre-coated with RNase-free yeast tRNA (Sigma, St. Louis, MO, USA) at 4°C for 3 hrs. The cells were washed twice with cold lysis buffer, thrice with low salt buffer solution and once with high salt buffer solution. Antagonism miR-23b-3p probe was used as negative control. qRT-PCR was applied to determine the expression of RP11-422N16.3.

Quantitative Reverse Transcript Polymerase Chain Reaction

Trizol (Invitrogen, Carlsbad, CA, USA) reagent was applied to extract the total RNA from tissue samples and cells. Ultraviolet analysis and formaldehyde denaturation electrophoresis were applied to verify the quality of extracted RNA. Then, 1 μg of RNA was subjected to AMV reverse transcriptase to obtain cDNA. PCR primers were designed and synthesized by Sangon Biotech (Shanghai, China) (Table 1). GAPDH was used as an internal control and U6 was used as an internal control for RNA in cell nucleus and miR-23b-3p. PCR was amplified with the following conditions: pre-denature at 94°C for 5 mins, followed by 40 cycles of denature at

Table 1 Primer Sequences for RT-PCR

Genes	Sequences
RP11-422N16.3	F:5'-CCGTAGGACTCGCAGGACTCG-3'
	R:5'-GGTGAGAGGTGAGCTGGTAAGGAG-3'
miR-23b-3p	F:5'-ACACTCCAGCTGGGATCACATTGCCAGGGAT-3'
	R:5'-CTCAACTGGTGTCGTGGAGTCGGCAATTCAGTTGAGGTGGTAAT-3'
DMGDH	F:5'-TCCATCGTCCACAGAAAG-3'
	R:5'-AAATGTCCTCCGCAAGCT-3'
U6	F:5'-GCTTCGGCAGCACATATACTAAAAT-3'
	R:5'-CGCTTCACGAATTTGCGTGTCAT-3'

94°C for 40s, anneal at 60°C for 40s and extend at 72°C for 1 min, and finally extend at 72°C for 10 mins. The PCR product was verified through agarose gel electrophoresis. The lowest point in the parallel rising of the logarithmic amplification curve was manually selected to obtain the cycle threshold. Data were analyzed by $2^{-\Delta\Delta Ct}$ method, in which $2^{-\Delta\Delta Ct}$ presents the ratio of gene expressions between the experimental group and the control group.

Western Blot

The proteins from cells and tissue samples in each group were extracted and measured using BCA kit (Wuhan Boster Biological Technology, Ltd). Loading buffer was added for boiling at 95°C for 10 mins. Thirty micrograms of proteins were separated in 10% polyacrylamide gel (Wuhan Boster Biological Technology. LTD). The resolving proteins were transferred into the PVDF membrane. The blocking was performed using 5% BSA at room temperature. The primary antibodies of DMGDH, E-cadherin, Vimentin (1:1000) and β-actin (1:3000) were purchased from Abcam Cambridge, MA, USA. The primary antibodies were added and incubated at 4°C overnight. Then, the membrane was washed thrice with TBST for 5mins. The corresponding secondary antibodies (Shanghai MT-bio, China) were added for incubation for 1 h at room temperature. The membrane was washed thrice for5-mins before color development. Bio-rad Gel Dol EZ imager (GEL DOC EZ IMAGER, Bio-Rad, California, USA) was used to obtain images. The intensity of the target strip was analyzed by ImageJ software. Each test was repeated thrice to obtain the average value.

CCK-8 Assay

Cell suspension in each group was diluted and inoculated in a 96-well plate with $1 \times 10^3/100\mu L$/well. Each group has 15 parallel wells. According to the incubation time, cells in each group were sub-grouped into five groups (0h, 24hrs, 48hrs, 72hrs and 96hrs), with each subgroup has three duplicate wells. The culture medium without cells adding CCK-8 was served as blank control. The plate was incubated at 37°C with 5% CO_2. A total of 10 μL of CCK-8 reagent (Sigma, St. Louis, MO, USA) was added in corresponding well at each time point for incubation for 4 hrs. Later, the optical density (OD) was measured using a microplate reader (Bio-Rad, USA) under 450 nm wavelength.

Flow Cytometry (FCM)

Cells in logarithmic growth phase of each group were digested with pancreatic enzymes and centrifuged. The

supernatant was removed and cells collected. After cells were washed twice with pre-cold PBS, centrifugation was performed at 1000 rpm for 5 mins. Then, the cell density was adjusted into 10^6/mL and a total volume of 200 μl cells were washed twice with 1 mL PBS before centrifugation. Cells were re-suspended in 100 ul of binding buffer and added with 2 μl of Annexin-V-FITC (20 ug/mL) for full mixture at ice without light exposure. About 15 mins later, cells were transferred into the testing tube and 300 μl of PBS was added. Each sample was added with 1 μl PI (50 ug/mL) before detection within 30 mins. Using AnnexinV as horizontal axis, PI as vertical axis, cells in upper left area were mechanical damaged cells, upper right area were late apoptotic cells or necrotic cells, lower left area were negative normal cells and lower right area were early apoptotic cells.

Cell Migration Assay

Matrigel diluent was paved in 24-well plates, then the plates were placed in room temperature with air drying for 30 mins. Cells were inoculated in the prepared plate and cultured in an incubator (37°C, 5%CO$_2$). When cells fully covered the plate bottom, a line was lightly drawn in each well with a sterilized tip, ensuring the width of each line was the same. A mark was left on the cap of the 24-well plates in order to make sure the same visual field in the photograph, and then photos were taken and recorded as 0 hr. After 24 hrs incubation at 37°C, cell culture fluids were suctioned out and discarded. The 24-well plate was washed 3 times with PBS to remove any cell debris caused by scratching. Then, the cells were put into serum-free medium for photographing, and recorded as 24 hrs. Photographs were taken with an Olympus Inverted Microscope (Olympus Optical Co., Ltd, Tokyo, Japan) with six visual fields at a fixed location. The migrated distance was calculated with the ImageTool software (Bechtel Nevada, Los Alamos Operations, USA). Migrated distance = (width at 0hr – width at 24hrs)/2.

Transwell Chamber Assay

Each Transwell chamber (Corning Glass Works, Corning, New York, USA) was added with matrigel (BD Biosciences, USA. 3.9 mg/mL, 60~80 μL), and incubated at 37°C. When the matrigel was coagulated, chambers were taken out and put into a 24-well plate. After the medium was pre-warmed in the incubator, the pre-warmed mediums (0.5 mL per chamber) were separately added into upper and lower chambers. Then, the chambers were put into the incubator for a 2-

hr hydration, followed by the liquid being suctioned out from upper and lower chambers and being discarded. The cell suspension (5×10^4 cells/mL) was prepared after digestion. A total of 0.5 mL complete medium was extracted and put into a 24-well plate, and then the hydrated chamber was transferred into the 24-well plate, avoiding bubble formation. A total of 0.5 mL cell suspension was extracted and put into the chamber, followed by incubation at 37°C for 24 hrs. The liquid in upper and lower chambers was suctioned out and discarded. Cotton swabs were used to clean the cells on the surface of the upper chamber of the Transwell membrane. After three PBS washed, the transferred cells were fixed with ice-cold methanol for 30 mins. Cells were then dyed with 0.1% crystal violet for 10 mins. After this, cells were washed with running water until no extra crystal violet remained and were air-dried. Finally, data were recorded through observation and photography under a microscope. Photographs were captured using an Olympus Inverted Microscope (Olympus Optical Co., Ltd., Tokyo, Japan) with six visual fields at a fixed location. A hit counter was applied to count the number of cells transferred onto Transwell lower chamber.

Statistical Analysis

SPSS 21.0 (SPSS, Inc, Chicago, IL, USA) software was used for data analysis. The obtained data were expressed as mean ± standard deviation. Data were analyzed using Kolmogorov–Smirnov if data were in normal distribution. Comparisons between two groups were analyzed using t-test, while comparisons among multi groups were analyzed through One-Way ANOVA. Pairwise comparison after ANOVA analysis was conducted using Fisher's least significant difference t-test (LSD-t). P value was based on a two-sided test. $P < 0.05$ was considered as statistical difference.

Results

Decreased LncRNA RP11-422N16.3 Expression in Hepatocellular Carcinoma Tissues and Hepatocellular Carcinoma Cells

Quantitative RT-PCR was applied to detect the expressions of RP11-422N16.3 in hepatocellular carcinoma tissues and adjacent normal tissues. The results showed that RP11-422N16.3 expression in hepatocellular carcinoma tissues was significantly decreased compared with adjacent normal tissues ($P < 0.01$) (Figure 1A).

RP11-422N16.3 expression was also reduced in hepatocellular carcinoma HepG2, SMMC-7721, MHCC97-H, and HCCLM3 cells in contrast to that in human normal
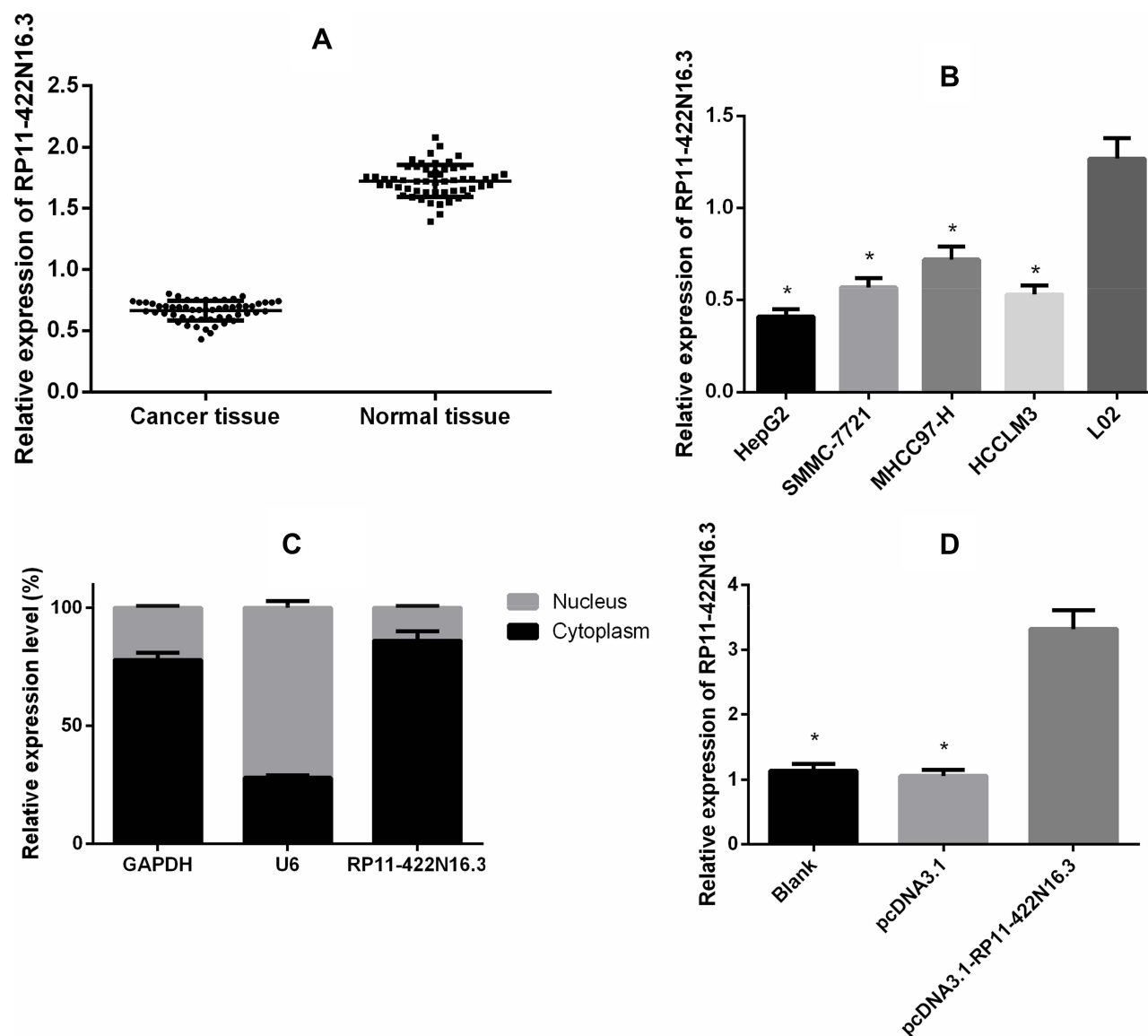
Figure 1 RP11-422N16.3 expressions in liver cancer tissue and cell lines. (**A**): relative RP11-422N16.3 expression in normal tissues and cancer tissues; (**B**): Relative RP11-422N16.3 expression in hepatocellular carcinoma cell lines (HepG2, SMMC-7721, MHCC97-H, and HCCLM3) and normal live cell line (L02); (**C**): RP11-422N16.3 expression in cytoplasm was higher than that in nucleus in subcellular fractionations; (**D**): overexpression of RP11-422N16.3 in HepG2 cell was successfully established. *Indicated that P < 0.05 compared to L02 or Blank group.

liver cell line (L02) cells (P < 0.05). Among the four hepatocellular carcinoma cell lines, HepG2 had the lowest RP11-422N16.3 expression (Figure 1B); therefore, HepG2 cells were selected for further experiments.

The localization of RP11-422N16.3 in HepG2 cells was investigated using subcellular fractionation. It was found that RP11-422N16.3 localized in cell nucleus and cytoplasm of HepG2 cells, with higher expression in cytoplasm than in nucleus, indicating an important role of RP11-422N16.3 in the cytoplasm of hepatocellular carcinoma cells (Figure 1C).

qRT-PCR results showed that in HepG2 cells, cells in pcDNA3.1-RP11-422N16.3 group had significantly higher

expression of RP11-422N16.3 than those in pcDNA3.1 group (P < 0.05) (Figure 1D), suggesting that overexpression of RP11-422N16.3 in HepG2 cells was successfully established.

Overexpression of RP11-422N16.3 Inhibits Proliferation and Promotes Apoptosis in Hepatocellular Carcinoma Cells

CCK-8 assay was applied to determine the effect of overexpression of RP11-422N16.3 on cell proliferation. The results demonstrated that there was no significant difference

in cell proliferation in pcDNA3.1 group compared with blank group (P > 0.05). However, cell proliferation in pcDNA3.1-RP11-422N16.3 group was inhibited (P < 0.05) (Figure 2A).

Cell apoptosis was examined with the application of FCM. The results suggested that there was no difference on cell apoptosis between blank groups and pcDNA3.1 group (P > 0.05). Cell apoptosis in pcDNA3.1-RP11-422N16.3 group increased in contrast to pcDNA3.1 group (P < 0.05) (Figure 2B and C). These results implied that overexpression of RP11-422N16.3 can inhibit proliferation and promote apoptosis in hepatocellular carcinoma cells.

Overexpression of RP11-422N16.3 Inhibits EMT in Hepatocellular Carcinoma

Under an inverted microscope, it was found that HepG2 cells in blank groups were fusiform similar to mesenchymal cells. The cells in pcDNA3.1 group were similar to that of blank groups, while cells in pcDNA3.1-RP11-422N16.3 group gradually changed to round shape (Figure 3A).

Western Blot was utilized to determine the expression of EMT-related proteins (ZEB1, Snail, E-cadherin and Vimentin). There was no difference in the expression of ZEB1 and Snail in blank groups and pcDNA3.1 groups of HepG2 cells (P > 0.05). In contrast, the expressions of ZEB1 and Snail in pcDNA3.1-RP11-422N16.3 group were substantially reduced compared to the pcDNA3.1 group (P < 0.05). There was no difference in the expression of E-cadherin and Vimentin in blank groups and pcDNA3.1 groups of HepG2 cells (P > 0.05). However, cells in pcDNA3.1-RP11-422N16.3 group showed elevated expression of E-cadherin, and decreased expression of Vimentin compared with cells in pcDNA3.1 group (P < 0.05) (Figure 3B). These results suggested that overexpression of RP11-422N16.3 inhibits EMT in hepatocellular carcinoma cells.

Overexpression of RP11-422N16.3 Inhibits Cell Migration and Invasion in Hepatocellular Carcinoma

Scratch test was performed to measure cell migration, results confirmed that at 0hr, the cells in all groups adhered well, and there was no cell adherence at the scratch; after 24hrs, the cells started to migrate to the middle of the scratch. The scratches of the blank, inhibitor NC and pcDNA3.1 groups were covered by cells, and the migrated distance of pcDNA3.1-RP11-422N16.3 and miR-23b-3p groups was significantly shorter than other groups, P < 0.05 (Supplementary Figure 4A).

Transwell chamber assay was performed to detect cell invasion. Results showed that the numbers of cell invasion in the blank, inhibitor NC and pcDNA3.1 groups were higher than that in the pcDNA3.1-RP11-422N16.3 and miR-23b-3p groups, P<0.05 (Supplementary Figure 4B).

It is suggested that overexpression of RP11-422N16.3 and down-regulation of miR-23b-3p can inhibit the migration and invasion of HepG2 cells.

Increased Expression of miR-23b-3p in Hepatocellular Carcinoma Tissues and Cells

qRT-PCR was applied to detect the expressions of miR-23b-3p in hepatocellular carcinoma tissues and adjacent normal tissues. The results showed that compared with adjacent normal tissues, hepatocellular carcinoma tissues had increased expression of miR-23b-3p (P < 0.05) (Figure 4A).

In comparison with normal L02 cells, miR-23b-3p expression in hepatocellular carcinoma cells (HepG2, SMMC-7721, MHCC97-H, and HCCLM3) was elevated (P < 0.05). Among the hepatocellular carcinoma cells, HepG2 had the highest miR-23b-3p expression (Figure 4B).

qRT-PCR detection showed that in HepG2 cells, expression of miR-23b-3p in miR-23b-3p inhibitors group was lower than those ininhibitors NC group (P < 0.05) (Figure 4C), indicating the successful establishment of low-expression of miR-23b-3p in HepG2 cells.

Down-Regulation of miR-23b-3p Inhibits Cell Proliferation and Promotes Cell Apoptosis in Hepatocellular Carcinoma

CCK-8 assay in HepG2 cells showed that cells transfected with miR-23b-3p inhibitors inhibited cell proliferation, while transfection with NC had no effect on cell proliferation (P < 0.05) (Figure 5A).

FCM showed that cell apoptosis rate in miR-23b-3p inhibitors group was elevated substantially, while there was no difference in cell apoptosis between blank group and NC group (P > 0.05). (Figure 5B). These results showed that down-regulation of miR-23b-3p inhibited cells proliferation and promoted cell apoptosis in hepatocellular carcinoma.

Down-Regulation of miR-23b-3p Inhibits EMT in Hepatocellular Carcinoma

Cell morphology was observed under an inverted microscope. HepG2 cells transfected with inhibitors NC showed no change in cell morphology. The cells transfected with
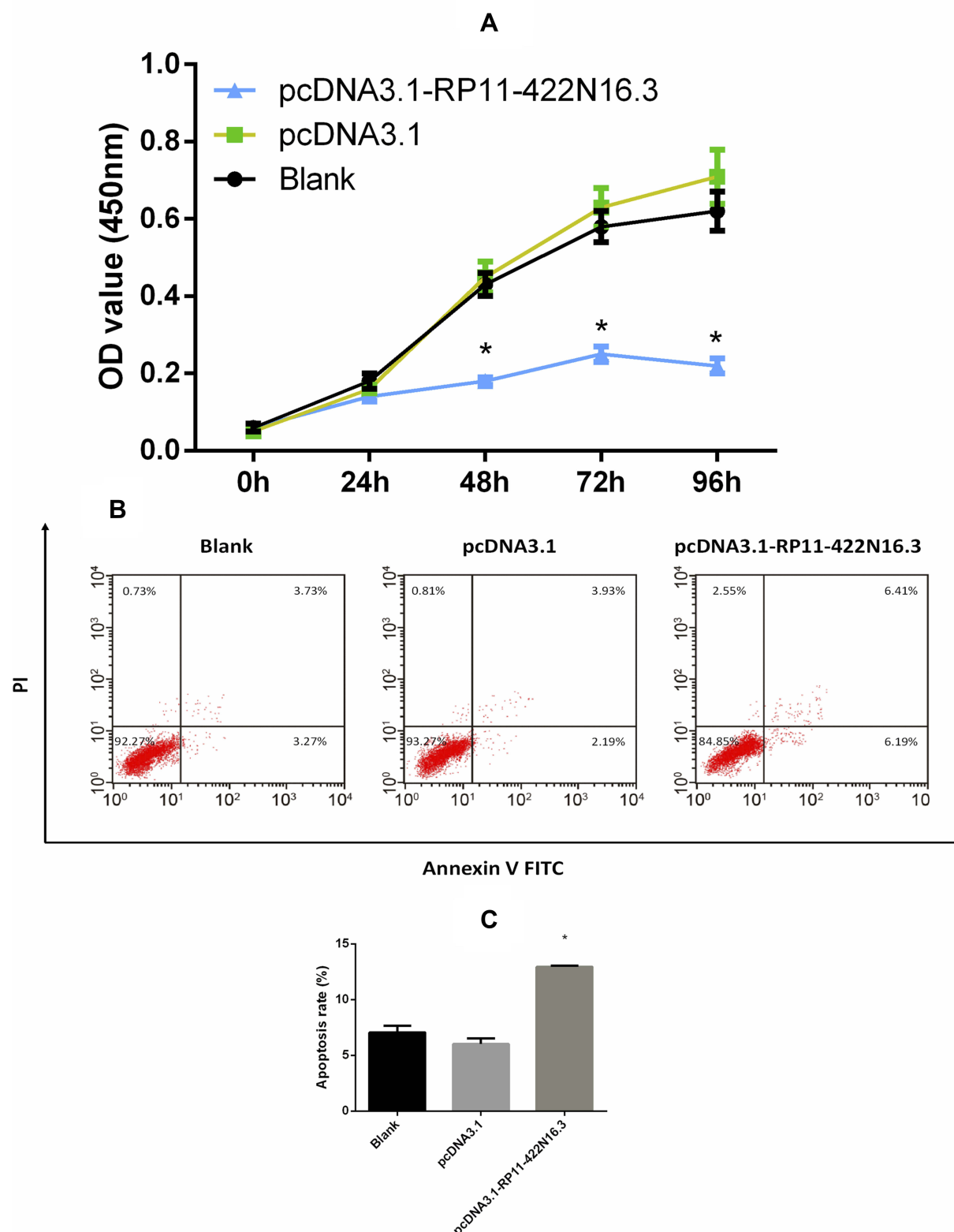
Figure 2 Effect of RP11-422N16.3 overexpression on HepG2 cell proliferation and apoptosis (**A**): CCK-8 assay showed that overexpression of RP11-422N16.3 could significantly inhibit cell proliferation ability; (**B** and **C**): flow cytometry showed that overexpression of RP11-422N16.3 could significantly promote cell apoptosis rate. *Indicated that P < 0.05 compared to blank group.
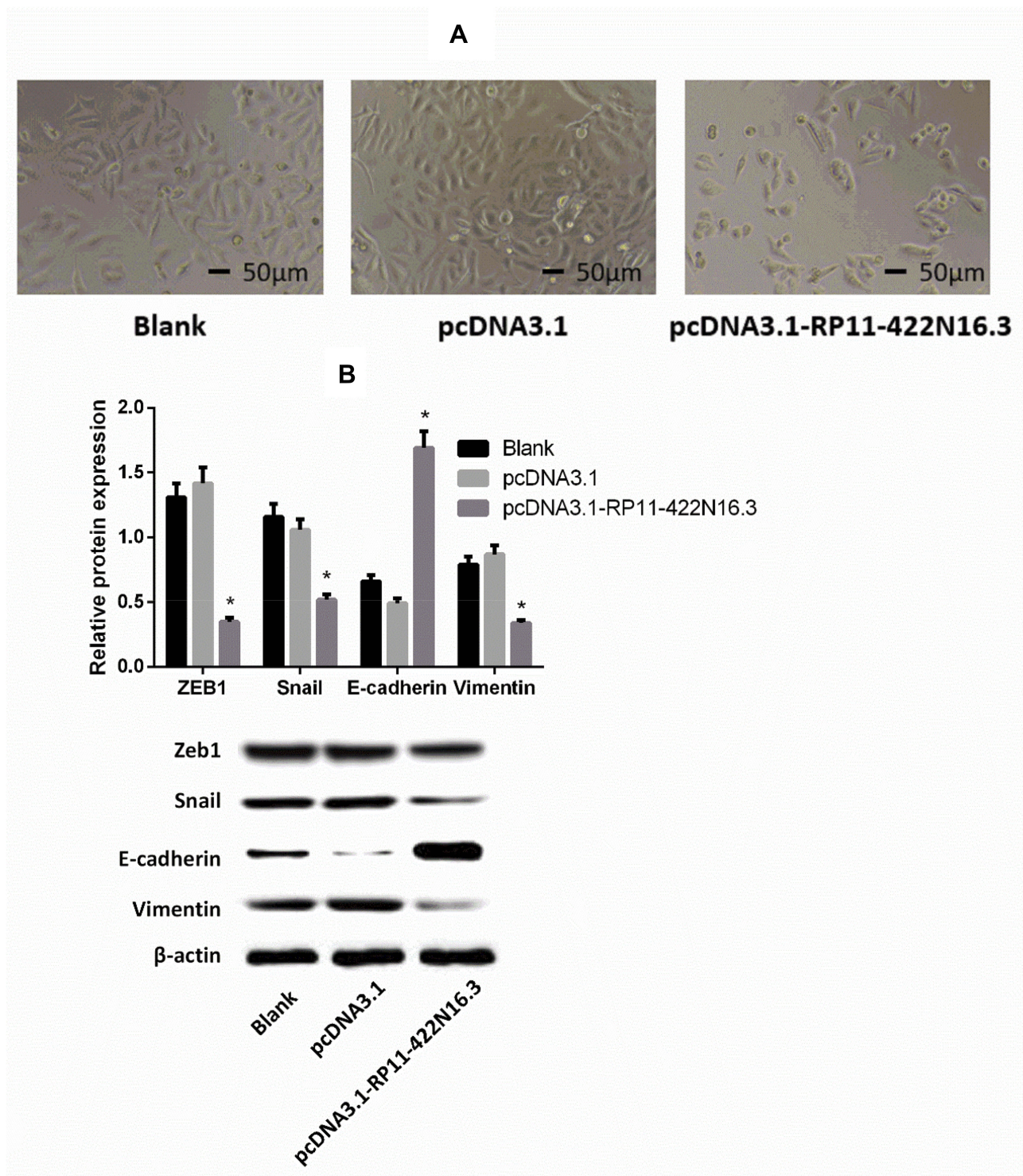
Figure 3 Overexpression of RP11-422N16.3 on EMT biomarkers in HepG2 cells. (**A**): cell morphology of HepG2 cells under an inverted microscope; (**B**): Western blot showed decreased ZEB1 and Snail expressions in cells of pcDNA3.1-PTENP1 group, and elevated expression of E-cadherin and decreased expression of Vimentin in cells of pcDNA3.1-PTENP1 group. *Compared with blank group, P < 0.05.

miR-23b-3p inhibitors gradually became round shape (Figure 6A).

Western Blot showed that there was no difference in expressions of ZEB1 and Snail in blank group and NC group in HepG2 cells (P > 0.05). In contrast to cells in NC group, the expressions of ZEB1 and Snail in miR-23b-3p inhibitors group were substantially reduced (P < 0.05). No significant difference on expressions of E-cadherin and
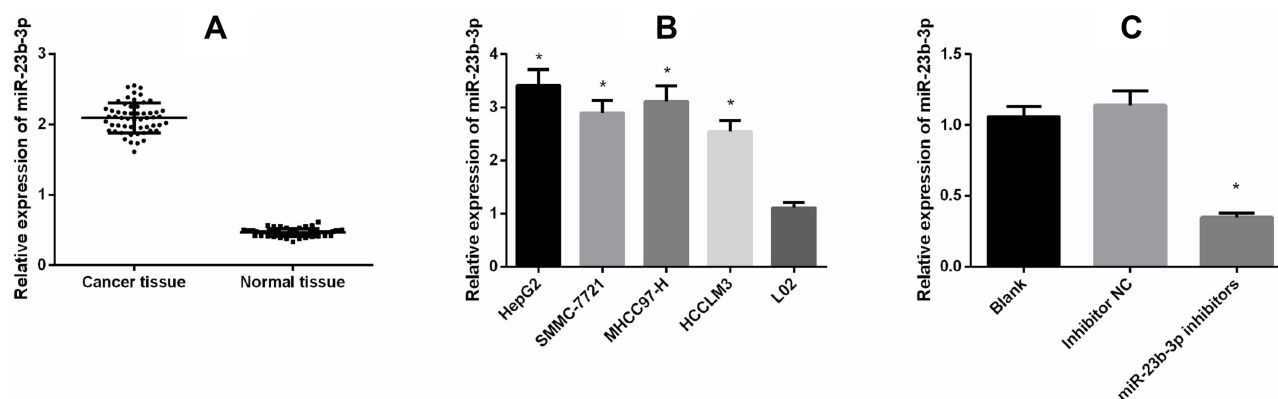
Figure 4 Mir-23b-3p expression in (**A**) cancer tissue and normal liver tissue, (**B**) hepatocellular carcinoma cell lines (HepG2, SMMC-7721, MHC97-H and HCCLM3) and normal liver cell line (L02) and (**C**) miR-23b-3p expression after cell transfection. *Indicated that P < 0.05 compared to blank or L02 groups.

Vimentin in HepG2 cells transfected with inhibitors NC (P > 0.05). Cells transfected with miR-23b-3p inhibitors had increased expression of E-cadherin, but decreased expression of Vimentin in HepG2 cells (P < 0.05) (Figure 6B).

Overexpression of miR-23b-3p Can Reverse the Effect of pcDNA3.1-RP11-422N16.3 on Cell Proliferation, Apoptosis and EMT in Hepatocellular Carcinoma

In HepG2 cells, cell proliferation in pcDNA3.1-RP11-422N16.3+miR-23b-3p mimics group increased compared to that in pcDNA3.1-RP11-422N16.3+mimics NC group (P < 0.05) (Figure 7A).

FCM showed that cell apoptosis in pcDNA3.1-RP11-422N16.3+miR-23b-3p mimics group was inhibited compared to that inpcDNA3.1-RP11-422N16.3+mimics NC group in HepG2 cells (P < 0.05) (Figure 7B).

Observation of cell morphology showed that HepG2 cells co-transfected with pcDNA3.1-RP11-422N16.3 and miR-23b-3p mimics changed to fusiform shape similar to mesenchymal cells (Figure 7C).

Western Blot confirmed that in HepG2 cells, the expressions of ZEB1 and Snail in pcDNA3.1-RP11-422N16.3+miR-23b-3p mimics group were substantially higher than that inpcDNA3.1-RP11-422N16.3+mimics NC group in HepG2 cells (P < 0.05) (Figure 7D), and the pcDNA3.1-RP11-422N16.3+miR-23b-3p mimics group had decreased expression of E-cadherin, and increased expression of Vimentin when compared with pcDNA3.1-RP11-422N16.3+mimics NC (P < 0.05) (Figure 7D). These results showed

that RP11-422N16.3 can regulate cell proliferation, apoptosis and EMT in hepatocellular carcinoma by targeting miR-23b-3p.

Overexpression of RP11-422N16.3 and Inhibition of miR-23b-3p Up-Regulated DMGDH expression

qRT-PCR and Western blot were applied to detect the mRNA and protein expression of DMGDH in hepatocellular carcinoma tissues and cells. The mRNA and protein expression of DMGDH in hepatocellular carcinoma tissues decreased compared with adjacent normal tissues (P < 0.05) (Figure 8A and B). The mRNA and protein expression of DMGDH in hepatocellular carcinoma cells decreased compared with normal hepatocellular cells (P < 0.05) (Figure 8C and D).

In HepG2 cells, the mRNA and protein expression of DMGDH in pcDNA3.1-RP11-422N16.3 group elevated when compared with pcDNA3.1 group. In addition, increased mRNA and protein expression of DMGDH was seen in miR-23b-3p inhibitors group compared with inhibitors NC group (P < 0.05) (Figure 8E and F).

RP11-422N16.3 Competitively Bound to miR-23b-3p to Promote DMGDH

The above results showed that there may be a negative targeting relationship between RP11-422N16.3 and miR-23b-3p in hepatocellular carcinoma tissues and cells. qRT-PCR further verified that the expression of miR-23b-3p in pcDNA3.1-RP11-422N16.3 group was inhibited when compared with pcDNA3.1 group, while the expression of RP11-422N16.3 in miR-23b-3p inhibitors group increased in
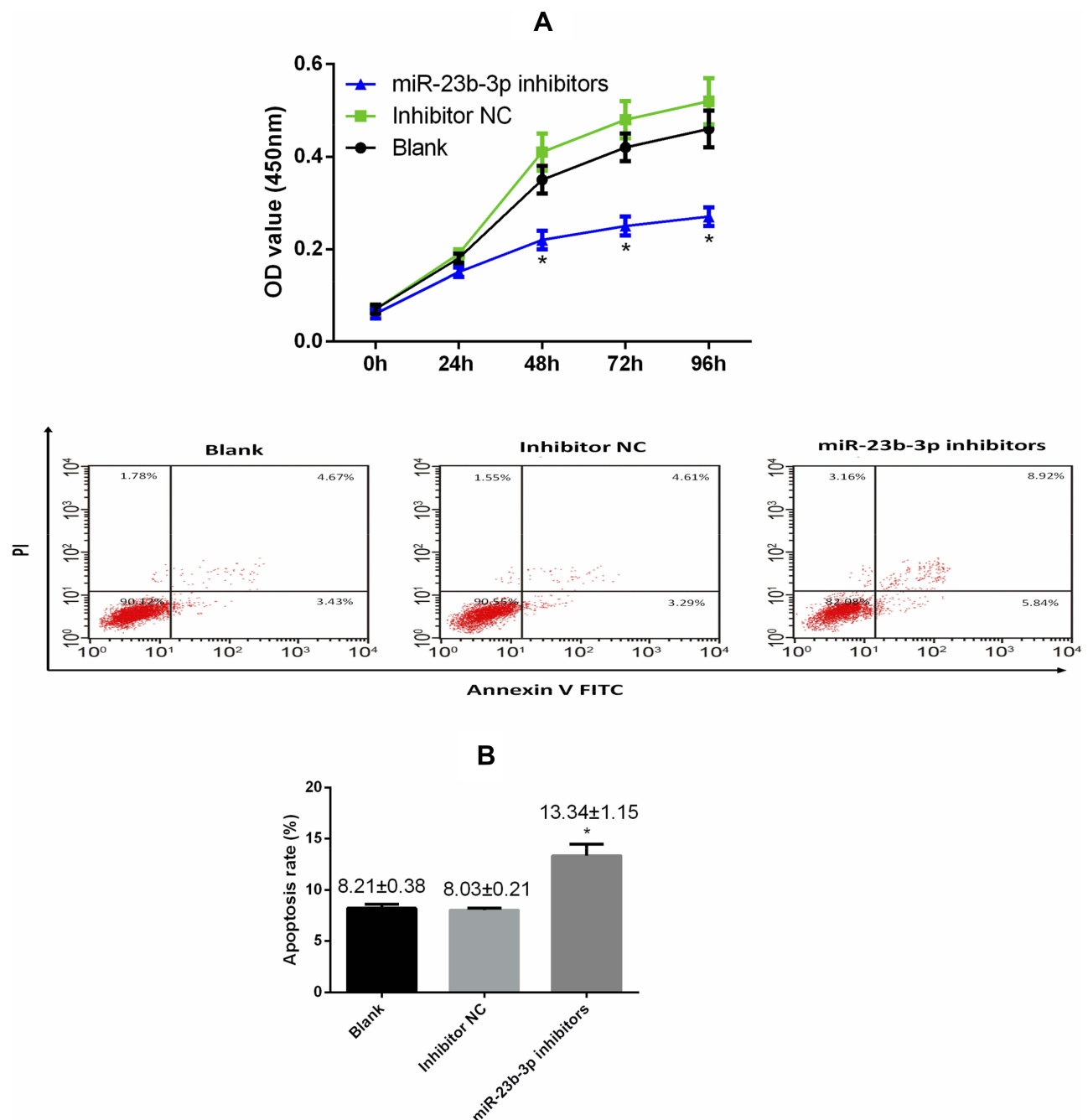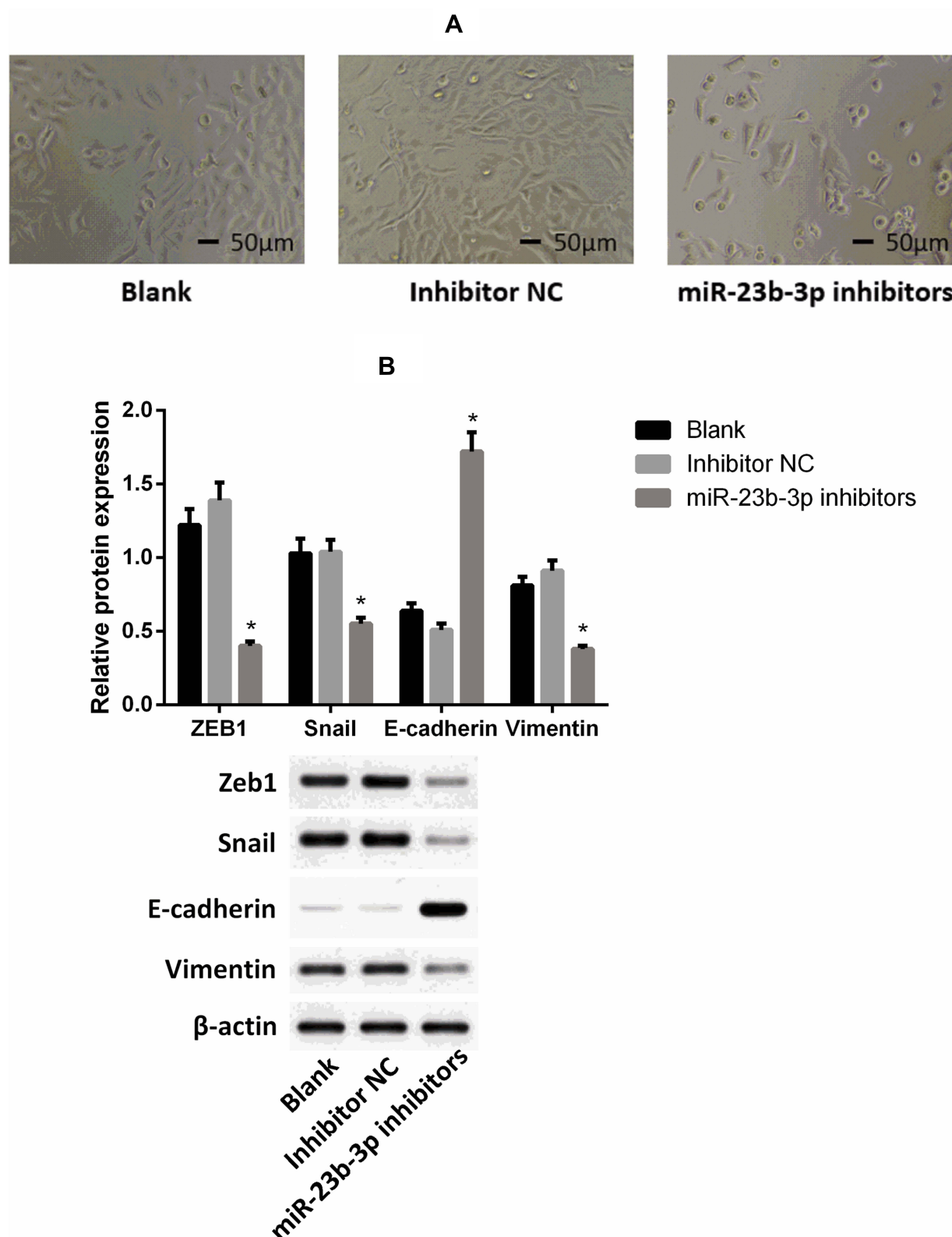
Figure 5 Effect of miR-23b-3p on HepG2 cell proliferation (**A**) and cell apoptosis (**B**), *Indicated that P < 0.05 compared to the blank group.

HepG2 cells compared withinhibitors NC group (P < 0.05) (Figure 9A and B).

Dual-luciferase reporter system identified that compared with mimics NC group, the luciferase activity of RP11-422N16.3+miR-23b-3p mimic group was inhibited (P < 0.05), while difference was found in comparison with mutant RP11-422N16.3+miR-23b-3p mimics group (P > 0.05). All these results supported the binding relationship between RP11-422N16.3 and miR-23b-3p (Figure 9C).

RNA-pull down assay in HepG2 cells showed that the expression of RP11-422N16.3 in Bio-miR-23b-3p-WT group was higher than that in Bio-probe NC group (P < 0.05). Comparison between Bio-miR-23b-3p-MUT group and Bio-probe NC group showed no difference (P > 0.05). Those data supported that Bio-miR-23b-3p-WT can gather RP11-422N16.3 around, which Bio-23b-3p-MUT cannot. RP11-422N16.3 can compete the binding site of miR-23b-3p, thus decreasing the activity of miR-23b-3p (Figure 9D).
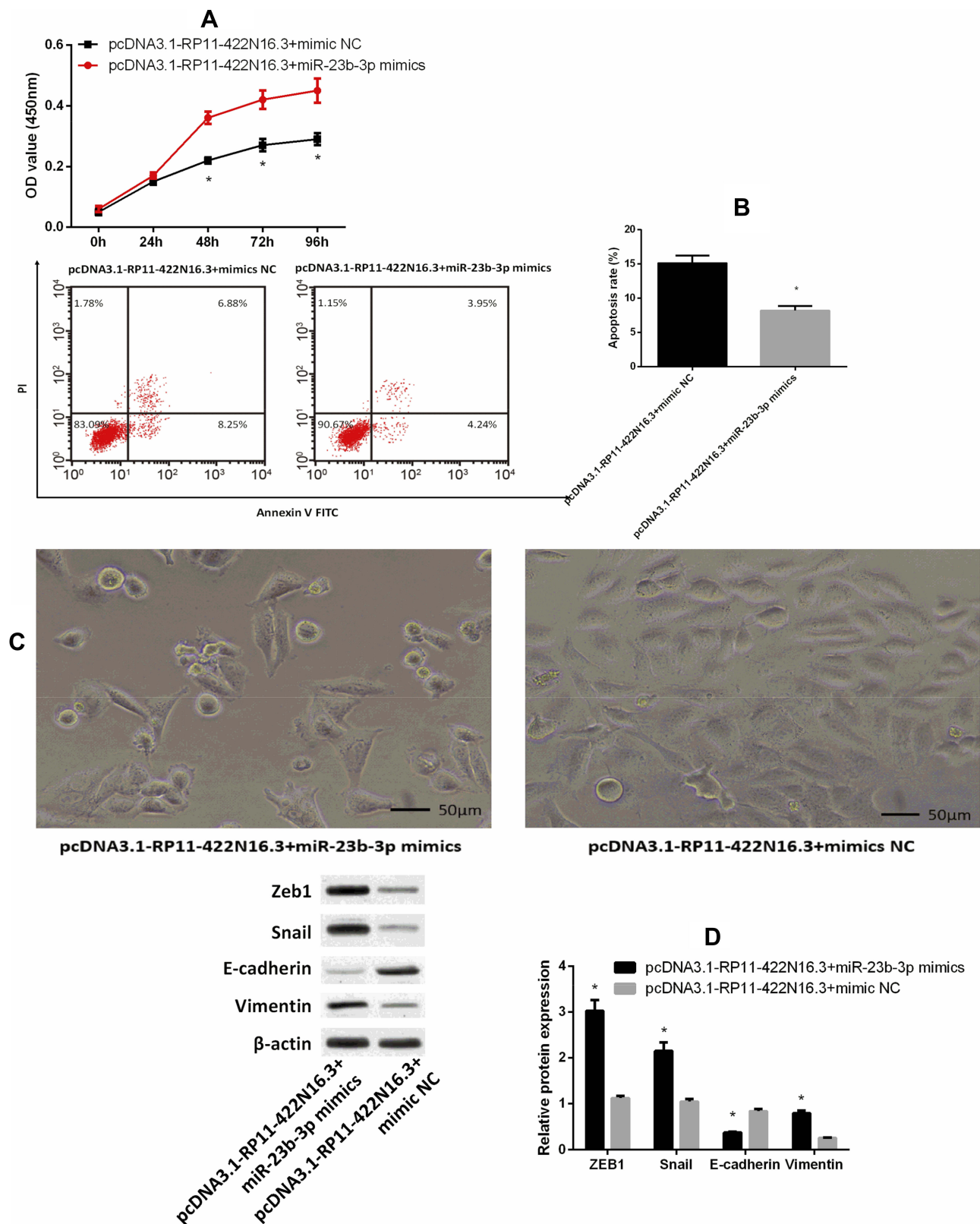
Figure 6 Effect of miR-23b-3p on HepG2 cell morphology (**A**) and EMT-related biomarker expressions (**B**). *Indicated that P < 0.05 compared to the blank group.

Target scan (http://www.targetscan.org) predicted that there is a targeting relationship between miR-23b-3p and DMGDH. Luciferase activity assay showed that compared with DMGDH-3′UTR-WT+mimics NC group, DMGDH-3′UTR-WT+ miR-23b-3p mimics had suppressed luciferase activity (P < 0.05). The luciferase activity of

Figure 7 Mir-23b-3p reversed the effect of RP11-422N16.3 on cell proliferation (**A**) and cell apoptosis (**B**). Observation of cell morphology showed that HepG2 cells co-transfected with pcDNA3.1-RP11-422N16.3 and miR-23b-3p mimics changed to fusiform shape similar to mesenchymal cells (**C**). miR-23b-3p reversed the effect of RP11-422N16.3 on EMT-related biomarker expressions (**D**). *Indicated that P < 0.05 compared to pcDNA3.1-RP11-422N16.3+mimic NC group.
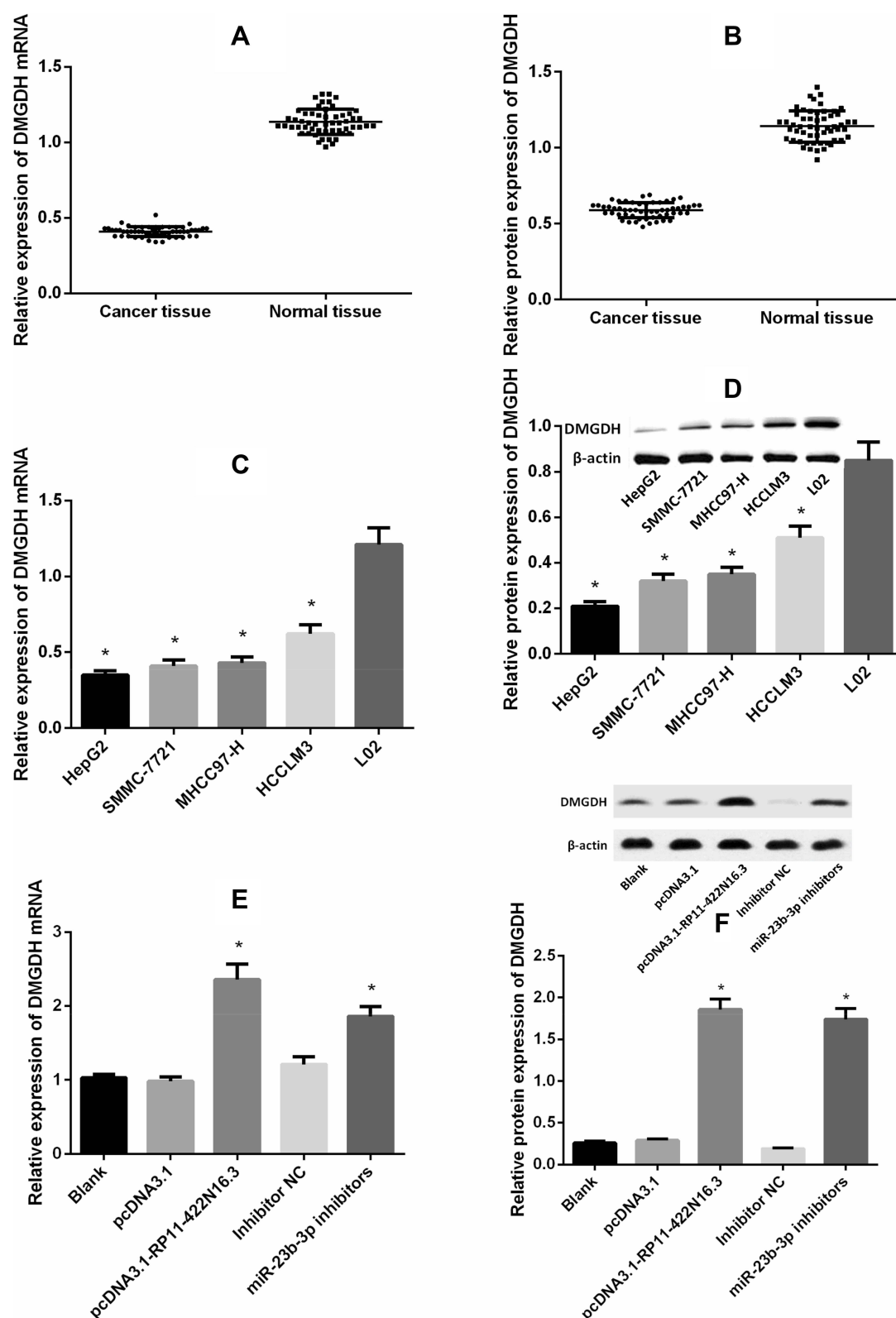
Figure 8 DMGDH expression in cancer tissue and normal tissue ((**A**): DMGDH mRNA expression; (**B**): DMGDH protein expression), and in hepatocellular carcinoma cell lines (HepG2, SMMC-7721, MHC97-H and HCCLM3) and normal liver cell line (L02) ((**C**): DMGDH mRNA expression; (**D**): DMGDH protein expression). Effect of RP11-422N16.3 and miR-23b-3p on DMGDH expression ((**E**): DMGDH mRNA expression; (**F**): DMGDH protein expression). *Indicated that P < 0.05 compared to Blank or L02 groups.
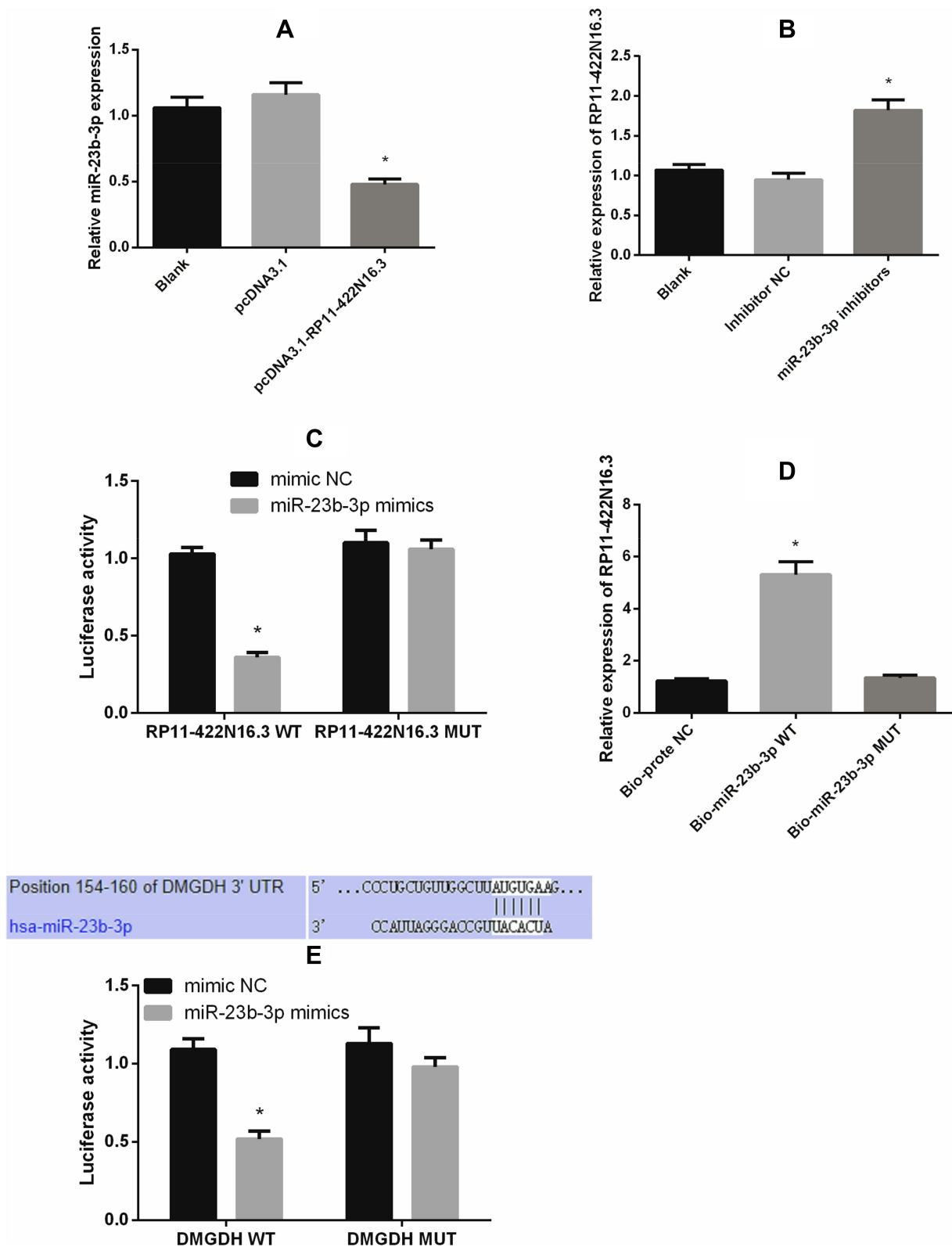
Figure 9 Overexpression of RP11-422N16.3 inhibited miR-23b-3p expression (**A**) and down-regulation of miR-23b-3p promoted RP11-422N16.3 expression (**B**). miR-23b-3p overexpression significantly reduced luciferase activity of wild type RP11-422N16.3, suggesting a potential targeting relationship between miR-23b-3p and RP11-422N16.3 (**C**). RNA-pull down assay showed binding relationship of miR-23b-3p and RP11-422N16.3 in HepG2 cell (**D**). Online software and luciferase activity assay confirmed the targeting relationship between miR-106b and PTEN (**E**); *Indicated that P < 0.05 compared to blank group, or NC group.

DMGDH-3′UTR-MUT+miR-23b-3p mimics was similar to that in DMGDH-3′UTR-MUT+mimics NC group (P > 0.05) (Figure 9E). All these data supported that DMGDH is a direct target gene of miR-23b-3p.

Discussion

It is estimated that approximately 93% of transcripts are lncRNAs, and lncRNAs are usually located in the nucleus and cytoplasm.[21] However, the gene transcription level of lncRNA is generally lower than that of protein-encoding genes, and the sequence conservation is poor. Compared with small RNAs (such as miRNAs), LncRNAs have longer sequences and more complex spatial structures, and the mechanisms involved in expression regulation are more diverse and complex. Abnormal expression of LncRNA is closely related to tumor diagnosis, recurrence, metastasis and prognosis.[22] LncRNAs display a variety of biological functions in cancer, and are widely involved in DNA damage repair, cell cycle regulation and other physiological or pathological processes to regulate tumor development, and can be used as transcriptional regulatory molecules of oncogenes and tumor suppressor genes. The mode of action can be roughly divided into four categories: signal, decoy, guide and scaffold.[23] LncRNAs can regulate the expression of genes through epigenetic regulation, transcriptional regulation and post-transcriptional regulation, and thus participate in various biological processes such as cell proliferation, differentiation and apoptosis in cancer, the role of LncRNAs in signaling pathways has become an important part of the mechanism of cancer development.[24,25] Lnc TCF7 is highly expressed in liver cancer cells and plays an important role in the maintenance of liver cancer stem cell self-renewal ability. Lnc TCF7 activates the Wnt signaling pathway by binding to and recruiting SWI/SNF complexes to bind to the promoter of the TCF7 gene to activate gene expression, which leads to the development of liver cancer tumors.[26] TGF-β promotes the metastasis of liver cancer cells through lncRNA-ATB.[27] miRNAs can be paired with target RNAs, resulting in inhibition of gene expression and inhibition of protein synthesis. lncRNAs can act directly or indirectly with microRNAs, causing them to lose regulatory function. In addition, lncRNAs can also participate in gene transcriptional processes mediated by DNA methylation, acetylation, etc. to regulate tumorigenesis. ncRNAs can regulate every aspect of cancer. Double luciferase reporter assay in current study provided evidence supporting the negatively target relationship of miR-23b-3p with

DMGDH. LncRNAs act as an endogenous "sponge" or ceRNA interacting with miRNA and exert their biological function by binding to their target genes.[28] To confirm whether lncRNA RP11-422N16.3 interacts with miR-23b-3p, we applied RNA-pull down assay and the results supported the binding relationship between RP11-422N16.3 and miR-23b-3p.

As early as the 1950s, Warburg reported that pyruvate, which decomposes glucose in tumor cells, was converted to lactic acid in the presence of oxygen, rather than in the mitochondria, and was later called the "Warburg effect."[29] Recent studies have further found that the key to rapid and long-term growth, proliferation and hypoxia tolerance of cancer cells was that they were different from the metabolic characteristics of normal cells; and the metabolic characteristics of tumor cells can be used to distinguish tumor cells from normal cells.[30,31] Common features of tumor metabolism include changes in glucose aerobic glycolysis, glutamine metabolism, tricarboxylic acid cycle, and anabolism, these characteristics may become a new development direction for the treatment of cancer, thereby avoiding and overcoming the genetic heterogeneity of tumors, and revealing the significance of research on the metabolism of substances in tumor cells.[32,33] Therefore, we previously performed a co-expression analysis of RP11-422N16.3 and a metabolic enzyme-related gene, and found that dimethylglycine dehydrogenase (DMGDH) was significantly positively correlated with RP11-422N16.3 expression, and low expression of DMGDH was a significant adverse factor in the prognosis of liver cancer patients. DMGDH has two splicing isoforms. Isomer 1 consists of 866 amino acid residues with a molecular weight of 96,811 Da; isomer 2 consists of 394 amino acid residues with a molecular weight of 45,079 Da. Among them, residues 19-398 and 775-866 were deleted.[19,34] In the 1950s and early 1960s, DMGDH was first identified and purified from rat liver.[35] DMGDH is a flavin adenine dinucleotide (FAD) and tetrahydrofolate (THF)-dependent mitochondrial matrix enzyme involved in choline degradation, one-carbon metabolism, and respiratory chain electron transport. DMGDH catalyzes the oxidative demethylation of dimethylglycine (DMG) to form sarcosine, and can convert sarcosine to glycine to a certain extent, and participate in choline degradation. Choline is an essential nutrient and a component of many important biomolecules, such as the membrane phospholipid phosphatidylcholine and the neurotransmitter acetylcholine.[36,37] In recent years, DMGDH catalytic product sarcosine has also attracted people's attention and has been used as a biomarker for invasive prostate

cancer.[38] Therefore, regulation of sarcosine levels and related enzymes has become the focus of research.

Our results also demonstrated the effect of overexpression of RP11-422N16.3 and down-regulation of miR-23b-3p on cell proliferation, apoptosis and EMT in liver cancer cells. miR-23b-3p has been specifically linked to various functions in different cancers through a cell-type-dependent manner.[39] In several kinds of tumors, miR-23b-3p was reported to act as a tumor inhibitor.[40] It was shown that the downregulation of miR-23b-3p in gastric carcinoma inhibited growth and invasion of gastric cancer cells through targeting Notch 2 and inhibiting its expression.[41] In addition, overexpression of RP11-422N16.3 and down-regulation of miR-23b-3p was believed to inhibit EMT in liver cancer as supported by increased expression of E-cadherin and decreased expression of Vimentin. Apart from that, EMT is considered to be one of the most important mechanisms of tumor cell invasion and metastasis, in which epithelial cells obtain mesenchymal and fibroblast-like properties.[42–44] Our study was consistent with this observation as overexpression of RP11-422N16.3 and down-regulation of miR-23b-3p can inhibit EMT in liver cancer cells.

Conclusion

In summary, this study elucidated that RP11-422N16.3 can competitively bind to miR-23b-3p to regulate expression of DMGDH. Overexpression of RP11-422N16.3 and inhibition on miR-23b-3p contributed to the suppression of cell proliferation and accelerating cell apoptosis in liver cancer cells. RP11-422N16.3 could be a potential therapeutic target for liver cancer.

Data Sharing Statement

The datasets used and/or analyzed during the current study are available from the corresponding author on reasonable request.

Author Contributions

Research concept and design: Qiandong Zhu, Collection and/or assembly of data: Qingqing Zhou, Data analysis and interpretation: Junjian Li, Writing the article: Yunpeng Sun, Critical revision of the article: Chang Zhao, Final approval of article: Zhengping Yu, Qiandong Zhu. All authors contributed to data analysis, drafting or revising the article, gave final approval of the version to be published, and agree to be accountable for all aspects of the work.

Ethics Approval and Informed Consent

This study was approved by the Ethics committee of The First Affiliated Hospital of Wenzhou Medical University.

Consent for Publication

All patients signed written informed consents and had the right to know the experiment prior to the study.

Funding

Disclosure

The authors report no conflicts of interest in this work.

References

1. Hartke J, Johnson M, Ghabril M. The diagnosis and treatment of hepatocellular carcinoma. *Semin Diagn Pathol*. 2017;34(2):153–159. doi:10.1053/j.semdp.2016.12.011
2. Wang Z, Luo Y. MicroRNA-367 promotes progression of hepatocellular carcinoma through PTEN/PI3K/AKT signaling pathway. *Biosci Rep*. 2019. doi:10.1042/BSR20182466
3. Gao H, Wang T, Zhang P, et al. Linc-ROR regulates apoptosis in esophageal squamous cell carcinoma via modulation of p53 ubiquitination by targeting miR-204-5p/MDM2. *J Cell Physiol*. 2019. doi:10.1002/jcp.29139
4. Shen JJ, Zhang CH, Chen ZW, et al. LncRNA HOTAIR inhibited osteogenic differentiation of BMSCs by regulating Wnt/beta-catenin pathway. *Eur Rev Med Pharmacol Sci*. 2019;23(17):7232–7246. doi:10.26355/eurrev_201909_18826
5. Li Q, Lei C, Lu C, Wang J, Gao M, Gao W. LINC01232 exerts oncogenic activities in pancreatic adenocarcinoma via regulation of TM9SF2. *Cell Death Dis*. 2019;10(10):698. doi:10.1038/s41419-019-1896-3
6. Feng H, Wei B, Zhang Y. Long non-coding RNA HULC promotes proliferation, migration and invasion of pancreatic cancer cells by down-regulating microRNA-15a. *Int J Biol Macromol*. 2019;126:891–898. doi:10.1016/j.ijbiomac.2018.12.238
7. Peng W, Gao W, Feng J. Long noncoding RNA HULC is a novel biomarker of poor prognosis in patients with pancreatic cancer. *Med Oncol*. 2014;31(12):346. doi:10.1007/s12032-014-0346-4
8. Yu F, Wang L, Zhang B. Long non-coding RNA DRHC inhibits the proliferation of cancer cells in triple negative breast cancer by down-regulating long non-coding RNA HOTAIR. *Oncol Lett*. 2019;18(4):3817–3822. doi:10.3892/ol.2019.10683
9. Ismail DM, Shaker OG, Kandeil MA, Hussein RM. Gene expression of the circulating long noncoding RNA H19 and HOTAIR in Egyptian colorectal cancer patients. *Genet Test Mol Biomarkers*. 2019;23(9):671–680. doi:10.1089/gtmb.2019.0066
10. Ji F, Wuerkenbieke D, He Y, Ding Y, Du R. Long noncoding RNA HOTAIR: an oncogene in human cervical cancer interacting with MicroRNA-17-5p. *Oncol Res*. 2018;26(3):353–361. doi:10.3727/096504017X15002869385155

11. Li N, Meng DD, Gao L, et al. Overexpression of HOTAIR leads to radioresistance of human cervical cancer via promoting HIF-1alpha expression. *Radiat Oncol*. 2018;13(1):210.

12. Guo X, Xiao H, Guo S, et al. Long noncoding RNA HOTAIR knockdown inhibits autophagy and epithelial-mesenchymal transition through the Wnt signaling pathway in radioresistant human cervical cancer HeLa cells. *J Cell Physiol*. 2019;234(4):3478–3489. doi:10.1002/jcp.26828

13. Xuan Y, Wang Y. Long non-coding RNA SNHG3 promotes progression of gastric cancer by regulating neighboring MED18 gene methylation. *Cell Death Dis*. 2019;10(10):694. doi:10.1038/s41419-019-1940-3

14. Mohr AM, Mott JL. Overview of microRNA biology. *Semin Liver Dis*. 2015;35(1):3–11. doi:10.1055/s-00000069

15. Tian T, Wang J, Zhou X. A review: microRNA detection methods. *Org Biomol Chem*. 2015;13(8):2226–2238. doi:10.1039/C4OB02104E

16. Lu TX, Rothenberg ME. MicroRNA. *J Allergy Clin Immunol*. 2018;141(4):1202–1207. doi:10.1016/j.jaci.2017.08.034

17. Zhou W, Xu J, Wang C, Shi D, Yan Q. miR-23b-3p regulates apoptosis and autophagy via suppressing SIRT1 in lens epithelial cells. *J Cell Biochem*. 2019;120:19635–19646.

18. Zhu R, Li X, Ma Y. miR-23b-3p suppressing PGC1alpha promotes proliferation through reprogramming metabolism in osteosarcoma. *Cell Death Dis*. 2019;10(6):381. doi:10.1038/s41419-019-1614-1

19. Liu G, Hou G, Li L, Li Y, Zhou W, Liu L. Potential diagnostic and prognostic marker dimethylglycine dehydrogenase (DMGDH) suppresses hepatocellular carcinoma metastasis in vitro and in vivo. *Oncotarget*. 2016;7(22):32607–32616. doi:10.18632/oncotarget.8927

20. Magnusson M, Wang TJ, Clish C, et al. Dimethylglycine deficiency and the development of diabetes. *Diabetes*. 2015;64(8):3010–3016. doi:10.2337/db14-1863

21. Ponting CP, Oliver PL, Reik W. Evolution and functions of long noncoding RNAs. *Cell*. 2009;136(4):629–641. doi:10.1016/j.cell.2009.02.006

22. Ramnarine VR, Kobelev M, Gibb EA, et al. The evolution of long noncoding RNA acceptance in prostate cancer initiation, progression, and its clinical utility in disease management. *Eur Urol*. 2019. doi:10.1016/j.eururo.2019.07.040

23. Xu J, Hu J, Xu H, et al. Long non-coding RNA expression profiling in biopsy to identify renal allograft at risk of chronic damage and future graft loss. *Appl Biochem Biotechnol*. 2019. doi:10.1007/s12010-019-03082-2

24. Liang H, Su X, Wu Q, et al. LncRNA 2810403D21Rik/Mirf promotes ischemic myocardial injury by regulating autophagy through targeting Mir26a. *Autophagy*. 2019;1–15.

25. Li K, Zhong S, Luo Y, et al. A long noncoding RNA binding to QKI-5 regulates germ cell apoptosis via p38 MAPK signaling pathway. *Cell Death Dis*. 2019;10(10):699. doi:10.1038/s41419-019-1941-2

26. Zhao J, Zhang L, Zheng L, Hong Y, Zhao L. LncRNATCF7 promotes the growth and self-renewal of glioma cells via suppressing the miR-200c-EpCAM axis. *Biomed Pharmacother*. 2018;97:203–208. doi:10.1016/j.biopha.2017.10.039

27. Tang F, Wang H, Chen E, et al. LncRNA-ATB promotes TGF-beta-induced glioma cells invasion through NF-kappaB and P38/MAPK pathway. *J Cell Physiol*. 2019;234(12):23302–23314. doi:10.1002/jcp.28898

28. Jia W, Jia S, Chen P, He Y. Construction and analysis of a long non-coding RNA (lncRNA)-associated ceRNA network in beta-thalassemia and hereditary persistence of fetal hemoglobin. *Med Sci Monit*. 2019;25:7079–7086. doi:10.12659/MSM.915946

29. Liberti MV, Locasale JW. The Warburg effect: how does it benefit cancer cells? *Trends Biochem Sci*. 2016;41(3):211–218. doi:10.1016/j.tibs.2015.12.001

30. Chen Z, Liu M, Li L, Chen L. Involvement of the Warburg effect in non-tumor diseases processes. *J Cell Physiol*. 2018;233(4):2839–2849. doi:10.1002/jcp.v233.4

31. Schwartz L, Supuran CT, Alfarouk KO. The Warburg effect and the hallmarks of cancer. *Anticancer Agents Med Chem*. 2017;17(2):164–170. doi:10.2174/1871520616666161031143301

32. Ma Y, Hu M, Zhou L, et al. Long non-coding RNA HOTAIR promotes cancer cell energy metabolism in pancreatic adenocarcinoma by upregulating hexokinase-2. *Oncol Lett*. 2019;18(3):2212–2219. doi:10.3892/ol.2019.10551

33. Chen S, Xu X, Lu S, Hu B. Long non-coding RNA HAND2-AS1 targets glucose metabolism and inhibits cancer cell proliferation in osteosarcoma. *Oncol Lett*. 2019;18(2):1323–1329. doi:10.3892/ol.2019.10445

34. Augustin P, Hromic A, Pavkov-Keller T, Gruber K, Macheroux P. Structure and biochemical properties of recombinant human dimethylglycine dehydrogenase and comparison to the disease-related H109R variant. *FEBS J*. 2016;283(19):3587–3603. doi:10.1111/febs.13828

35. Brizio C, Brandsch R, Douka M, Wait R, Barile M. The purified recombinant precursor of rat mitochondrial dimethylglycine dehydrogenase binds FAD via an autocatalytic reaction. *Int J Biol Macromol*. 2008;42(5):455–462. doi:10.1016/j.ijbiomac.2008.03.001

36. Luka Z, Pakhomova S, Loukachevitch LV, Newcomer ME, Wagner C. Folate in demethylation: the crystal structure of the rat dimethylglycine dehydrogenase complexed with tetrahydrofolate. *Biochem Biophys Res Commun*. 2014;449(4):392–398. doi:10.1016/j.bbrc.2014.05.064

37. McAndrew RP, Vockley J, Kim JJ. Molecular basis of dimethylglycine dehydrogenase deficiency associated with pathogenic variant H109R. *J Inherit Metab Dis*. 2008;31(6):761–768. doi:10.1007/s10545-008-0999-2

38. Heger Z, Merlos Rodrigo MA, Michalek P, et al. Sarcosine up-regulates expression of genes involved in cell cycle progression of metastatic models of prostate cancer. *PLoS One*. 2016;11(11):e0165830. doi:10.1371/journal.pone.0165830

39. Rezaei Z, Sebzari A, Kordi-Tamandani DM, Dastjerdi K. Involvement of the dysregulation of miR-23b-3p, miR-195-5p, miR-656-5p, and miR-340-5p in trastuzumab resistance of HER2-positive breast cancer cells and system biology approach to predict their targets involved in resistance. *DNA Cell Biol*. 2019;38(2):184–192. doi:10.1089/dna.2018.4427

40. Sun Q, Li J, Jin B, Wang T, Gu J. Evaluation of miR-331-3p and miR-23b-3p as serum biomarkers for hepatitis c virus-related hepatocellular carcinoma at early stage. *Clin Res Hepatol Gastroenterol*. 2019. doi:10.1016/j.clinre.2019.03.011

41. Xian X, Tang L, Wu C, Huang L. miR-23b-3p and miR-130a-5p affect cell growth, migration and invasion by targeting CB1R via the Wnt/beta-catenin signaling pathway in gastric carcinoma. *Onco Targets Ther*. 2018;11:7503–7512. doi:10.2147/OTT.S181706

42. Liao TT, Yang MH. Revisiting epithelial-mesenchymal transition in cancer metastasis: the connection between epithelial plasticity and stemness. *Mol Oncol*. 2017;11(7):792–804. doi:10.1002/1878-0261.12096

43. Du B, Shim JS. Targeting Epithelial-Mesenchymal Transition (EMT) to overcome drug resistance in cancer. *Molecules*. 2016;21(7). doi:10.3390/molecules21070965

44. Li L, Li W. Epithelial-mesenchymal transition in human cancer: comprehensive reprogramming of metabolism, epigenetics, and differentiation. *Pharmacol Ther*. 2015;150:33–46. doi:10.1016/j.pharmthera.2015.01.004